Bulletin of the Seismological Society of America, Vol. 105, No. 2A, pp. 497–510, April 2015, doi: 10.1785/0120140200

Review: Tilt-Free Low-Noise Seismometry

by Fabrice Matichard* and Matthew Evans

Abstract Inertial instruments used to measure horizontal motion are sensitive to tilt. Tilt coupling induced by gravity exerting a force along the sensing axis of the instrument as a function of its inclination must be accounted for in numerous seismological studies and seismic isolation applications. There are, in theory, many ways to separate tilt and horizontal motion components by combining the measurements of several sensors, and produce tilt-free estimations of the horizontal motion. This article reviews these configurations and analyses limitations related to sensor noise and geometrical couplings. It concludes with a discussion on the use of suspension mechanisms as an alternative to signal subtraction methods.

Introduction

Inertial sensors such as geophones, seismometers, and accelerometers used to measure translational acceleration are also sensitive to tilt due to the effect of gravity on the proof-mass of the instrument. Collette *et al.* (2012) reviews inertial sensors and points out the tilt-horizontal coupling effects affecting these instruments at low frequencies. Tilt-horizontal coupling induced by gravity on horizontal inertial sensors has been studied and discussed for more than a century. Wielandt and Forbriger (1999) provide a summary, including discussions that animated the seismological community during the late nineteenth century regarding the contribution of tilt effects in horizontal seismograms. Tilt effects in far field of earthquakes have been well understood and modeled for several decades. Rodgers (1968, 1969) discussed the effect of tilt motion on the horizontal pendulum seismometer. He analyzed the instrument's response for different types of wave motions, including Rayleigh waves, Love waves, and free oscillations of the Earth. He expressed correction factors to account for the tilt contribution in Rayleigh waves as a function of the wave's ellipticity, phase velocity, and period. This topic remains of interest as explained in recent publications. Peters (2009) assumes the vertical component is about 50% greater than the horizontal component of Rayleigh waves to estimate the frequencies at which tilt signal dominates over translational signal.

The tilt-coupling effect remains a significant issue in many applications even though it is well understood. Anthropogenic activity and winds are well-known causes of tilt effects masking low-frequency seismic data of interest. Forbriger (2006) points out the tilt effects observed in the urban environment, Lambotte *et al.* (2006) discusses tilt effects in long-period observations, and Wielandt and Forbriger (1999) analyze tilt effects in volcano seismology. The latter assume that the vertical and tilt components have the same waveform to decompose the motions through least-square minimization. Two vertical instruments are used over a long baseline to estimate the regional tilt. The authors show that the tilt contribution is significant, and they emphasize difficulties related to local tilt. Ground tilt significantly contributes to seismograms in the near zone of earthquakes and explosions. Graizer (2006) reviews these effects and develops a method based on comparison of horizontal and vertical components of seismograms to estimate the tilt contribution. More information on this topic can be found in Kalkan and Graizer (2007). Graizer (2005) shows that ignoring tilt effects may lead to unreliable calculation of long-period displacements. This is also demonstrated in the analysis and experimental work of Boroschek and Legrand (2006) on quasistatic components. Pillet and Virieux (2007) discuss these effects both for near-field and far-field measurements. Pillet *et al.* (2009) explains that ocean-bottom seismometers are significantly affected by these tilt effects. Tilt noise in seafloor seismic observations is also discussed by Crawford and Webb (2000). He emphasizes the role of seafloor compliance and the importance of the leveling for the vertical components. At low frequencies, he shows how the horizontal components and pressure measurements can be used to remove tilt from the vertical components. Zürn *et al.* (2007) also correlates changes of barometric pressure with tilt signal in horizontal seismograms.

Beyond seismological studies, tilt-horizontal coupling has become a limiting factor in the performance of seismic isolation and in vibration isolation applications. Inertial sensors are commonly used to actively isolate platforms and systems from ground motion. They have been used for several decades in research experiments. Notable examples include high-accuracy measurements of the Earth's gravitational field (see for instance Nelson, 1991), atom interferometry (Hensley *et al.*, 1999), and atomic force microscopy (see

*Also at LIGO Laboratory, California Institute of Technology, MS 100-36, Pasadena, California 91125.

for instance Kim *et al.*, 2009). Active inertial isolation has been studied for subsystems of large scale experiments (Artoos *et al.*, 2009; Collette *et al.*, 2011). Active seismic isolators have been developed and used for gravitational waves detectors for over three decades. Early concepts were presented by Robertson *et al.* (1982), discussed by Saulson (1984), and prototypes were developed at Joint Institute for Lab Astrophysics (Newell *et al.*, 1997; Richman *et al.*, 1998). Active inertial control has been implemented at the Virgo gravitational waves detector (Losurdo *et al.*, 2001) and for the initial Laser Interferometer Gravitational-Wave Observatory (LIGO; Hardham *et al.*, 2004; Hua *et al.*, 2004; Wen, 2009). The seismic isolation concept for Advanced LIGO detectors was presented in Abbott *et al.* (2002). The status of design and performance was summarized in Matichard *et al.* (2010, 2012, 2013). Both industrial and research applications aim for more isolation performance at lower frequencies. For most experiments, it is very difficult to provide active inertial isolation below 100 mHz. Tilt coupling is one of the main limiting factors, as explained by Lantz *et al.* (2009).

The goal of this article is to review the techniques commonly used to separate translation signal from tilt signal and to discuss limitations related to sensor noise. The next section gives a description of the physics of tilt-coupling effects induced by gravity on inertial horizontal sensors. The following section emphasizes the difference between tilt-horizontal coupling induced by gravity and tilt coupling induced by geometric couplings. The next one discusses techniques to reduce tilt-horizontal couplings in translation stages and points out that they are not effective for ground tilt effects. The following section reviews the limitations of tilt-subtraction methods and relates the tilt-coupling problem to sensor noise. The penultimate section reviews combinations of multiple instruments to separate tilt and translation motion. The final section discusses the use of suspensions to filter ground-motion transmission and to perform measurements independently of the support frame.

Tilt-Horizontal Coupling Induced by Gravity

Ratio of Sensitivities

There are several papers that describe the tilt-horizontal coupling effects induced by gravity (see Lantz *et al.*, 2009). In this article, a passive geophone model is used to introduce the problem, as shown in Figure 1. We assume that the periods of observation are sufficiently short to consider that the magnitude and direction of gravity are constant. The instrument is sensitive to two types of input motion: translation acceleration ($\ddot{x}$) and angular tilt (θ). It is made of a case connected to the ground (or a platform), the horizontal inertial motion of which is being measured. A mass mounted on a spring-damper moves with respect to the case in the sensing direction. The relative motion of the case with respect to the mass is called δ (we will use case motion minus mass motion

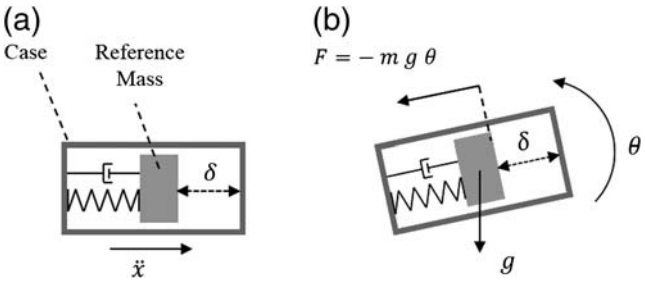

Figure 1. Horizontal inertial sensor subjected to (a) acceleration and (b) tilt.

as the sign convention). An electromechanical conversion translates this relative motion into a voltage. The converter usually also provides the internal damping. Geophones output signals are usually proportional to velocity above the natural frequency of the instrument. To study the tilt-horizontal coupling effect, it is convenient and sufficient to analyze the instrument's internal motion (δ) in displacement units.

In the following equations and in the article in general, we assume that the motions and angles are small. Small angle approximations are made (sine and tangent are approximated by the angle). The double dot above the variable represents the second time derivative. The study is performed in the Laplace domain. We often use the words ground motion in the text and we use displacement units in the equations, assuming that it is implicit that only second derivatives (acceleration) of the ground's translational motion can produce inertial signal.

The complex amplitudes of the input translation and rotation are called $\tilde{x}$ and $\tilde{\theta}$, respectively in equations (1) and (2). The complex amplitude of the instrument output is $\tilde{\delta}$ in equation (3). For simplicity, we use the same symbol (Ω) for the frequency of the input translation and the input rotation, but we assume that they are not necessarily correlated. They can be partially or well correlated in some cases (see Rodgers, 1968, for far-field, Wielandt and Forbriger, 1999, for near-field, and the Tilt Horizontal Coupling in Translation Stages and Vibration Isolation Systems section for seismic isolation), but they are not in most of the problems for which it is difficult to separate translation from tilt signal.

$$x(t) = \tilde{x}e^{i\Omega t}, \tag{1}$$

$$\theta(t) = \tilde{\theta}e^{i\Omega t}, \tag{2}$$

$$\delta(t) = \tilde{\delta}e^{i\Omega t}. \tag{3}$$

For simplicity, we will use the notations x, θ, and δ instead of $\tilde{x}$, $\tilde{\theta}$, and $\tilde{\delta}$ in the following developments to denote the complex values. The same convention will be used in all the analysis performed in the article. The instrument's response is written in the Laplace domain, in which the Laplace variable is called s ($s = i\Omega$). The response to translation,

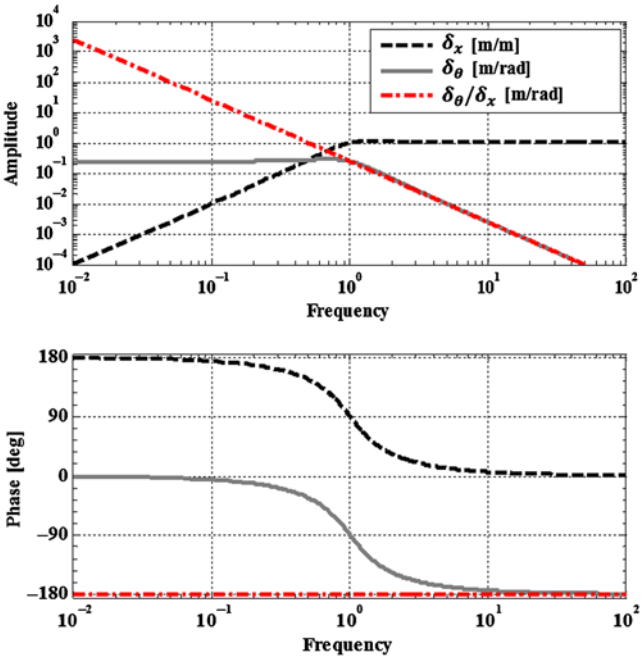

Figure 2. Horizontal seismometer sensitivity to translation (δ_x), tilt (δ_θ), and ratio of sensitivities (δ_x/δ_θ). The color version of this figure is available only in the electronic edition.

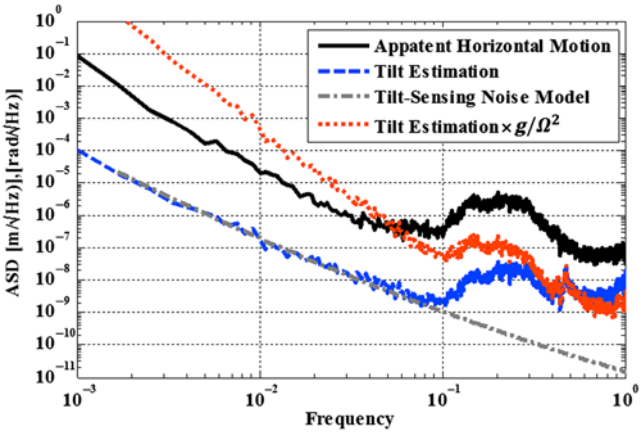

Figure 3. Example of tilt contribution estimates using broadband seismometers. The color version of this figure is available only in the electronic edition.

also called translation sensitivity, is δ_x. It is given by the transfer function in equation (4). The response to rotation, also called tilt sensitivity, is δ_θ. It is given by the transfer function in equation (5). The denominator is the same for the two transfer functions. It represents the geophones dynamics in which ω_s is the natural frequency and μ is the instrument's damping ratio. The numerators show the sensitivity to input motion. The translation sensitivity is proportional to s^2 (second derivative, acceleration), whereas the rotation sensitivity is directly proportional to gravity.

$$\delta_x = \frac{\delta}{x} = \frac{s^2}{s^2 + 2\mu\omega_s s + \omega_s^2}, \tag{4}$$

$$\delta_\theta = \frac{\delta}{\theta} = \frac{\mathrm{g}}{s^2 + 2\mu\omega_s s + \omega_s^2}. \tag{5}$$

The ratio of sensitivities is given in equation (6). The curves in Figure 2 show the frequency response of a typical geophone (1 Hz natural frequency, damping ratio of 0.5). The dashed line shows the translation sensitivity (δ_x), the solid line shows the tilt sensitivity (δ_θ), the dashed-dotted line shows the ratio of sensitivities. The lower the frequency, the more the tilt signal tends to dominate over the translation signal. Therefore, at very low frequencies, horizontal inertial instruments tend to act as tilt sensors. At high frequencies, they tend to act as a translation (acceleration) sensors. The frequency-dependent dual sensitivity of these instruments makes it difficult to analyze seismic motion and perform seismic isolation in the frequency band in which translation and tilt both contribute.

$$\frac{\delta_\theta}{\delta_x} = -g/\Omega^2. \tag{6}$$

Introductory Example

Tilt-horizontal confusion typically arises below 100 mHz, though it depends on the characteristics of the input motions. An example is given in Figure 3, for a measurement performed at the LIGO Livingston site. It uses broadband seismometers (Trillium T240) attached to a rigid structure operating in a vacuum. More information regarding this LIGO platform is given in the Multiple Instruments Configurations to Subtract Tilt section. The solid line shows the amplitude spectral density measured with the horizontal axis. It is calibrated in displacements units. The low-frequency part of the spectra is likely dominated by tilt coupling (motions amplitudes of 10^{-1} m/$\sqrt{\mathrm{Hz}}$ are not due to horizontal translation motion). An estimation of the tilt can be performed by combining the measurements of vertical seismometers. The tilt estimation can then be translated in equivalent horizontal signal induced by tilt coupling. The dashed curve shows the tilt motion estimated using the vertical axis of the broadband seismometers. It is calibrated in radian units. A model of the tilt sensing noise is shown by the dashed-dotted line. In this example, the tilt estimate is limited by sensor noise below 100 mHz. Sensor noise limitations related to such tilt estimates techniques are further discussed in the Multiple Instruments Configurations to Subtract Tilt section. The dotted curve translates this tilt estimation obtained with the vertical instruments into equivalent horizontal signal induced by tilt coupling (tilt estimation $\times\, \mathrm{g}/\Omega^2$). Below 50 mHz, the tilt estimation significantly overestimates the actual tilt contribution to the horizontal signal. This introductory example illustrates how sensor noise limits the possibilities to separate tilt from horizontal contributions in horizontal signals.

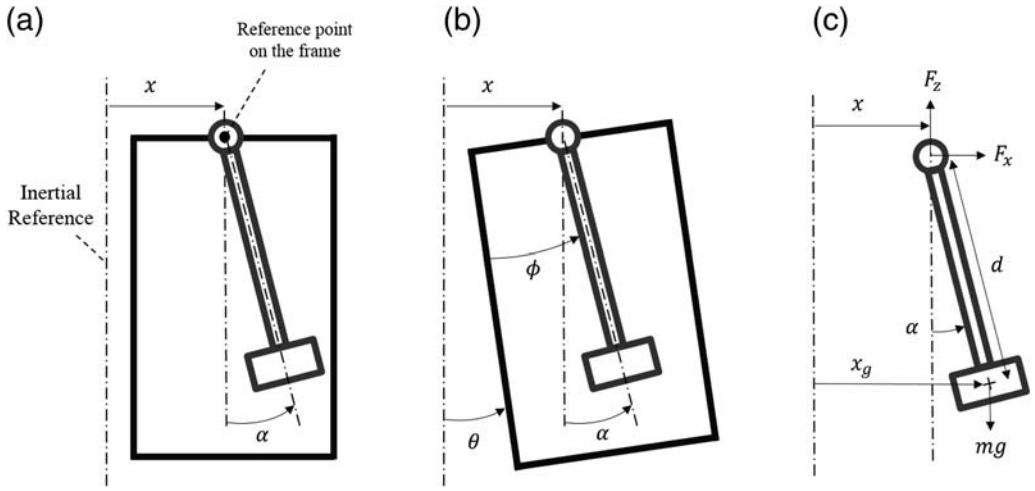

Figure 4. Pendulum seismometer: (a) input translation, (b) case rotation, and (c) forces and geometric parameters.

Instruments Topology

Although the model of a geophone has been used to describe the tilt-gravity coupling, similar effects occur in horizontal inertial instruments using different topologies such as pendulum seismometers, force feedback seismometers, and accelerometers. To illustrate this, a pendulum seismometer is used as another example as shown in Figure 4. The pendulum rotation α is induced by the input motion x as illustrated in Figure 4a. This motion can be estimated by measuring the rotation between the pendulum and the case (ϕ). Such measurement is sensitive to the frame's rotation, as shown in Figure 4b, because ϕ measures the differential rotation between the frame and the pendulum. Similar effects occur if a translation motion measurement is performed between the mass and the frame instead of measuring ϕ.

The equations of motion are written to compare the translation and the tilt contributions. The reference point is the center of the hinge. Equation (7) gives the motion of the center of mass x_g, as a function of the input translation x, the pendulum angle with respect to the inertial frame α, and the distance between the hinge and the center of mass d. The external forces on the pendulum are shown in Figure 4c. The horizontal force F_x accelerates the center of mass (mass m) as shown in equation (8). The vertical force F_Z equilibrates the force of gravity (acceleration g) as shown in equation (9). The sum of the moments around the center of mass is given in equation (10). Equations (7)–(10) are combined to obtain the pendulum response to the translation given in equation (11).

$$x_g = x + d\alpha, \tag{7}$$

$$F_x = m\ddot{x}_g, \tag{8}$$

$$F_Z = mg, \tag{9}$$

$$-F_x d - F_Z d\alpha = I\ddot{\alpha}, \tag{10}$$

$$\frac{\alpha}{x} = \frac{-mds^2}{(I + md^2)s^2 + mgd}. \tag{11}$$

In this example, the instrument's readout is the differential angle as shown in equation (12). The translation sensitivity is given by equation (13) (pure translation, $\theta = 0$), and the rotation sensitivity is given by equation (14). The ratio of sensitivity is given in equation (15). At low frequencies, the ratio of sensitivities tends toward g/s^2, as for a geophone. At high frequencies the ratio depends on the inertia and geometrical parameters. This is further discussed in the Using Very Low-Noise Rotation Sensors section. Detailed information can be found in Forbriger (2009) regarding the influence of the reference point's location on the instrument's sensitivity. Peters (2009) provides a detailed review and analysis of such instruments.

$$\phi = \alpha - \theta, \tag{12}$$

$$\phi_x = \frac{\phi}{x} = \frac{-mds^2}{(I + md^2)s^2 + mgd}, \tag{13}$$

$$\phi_\theta = \frac{\phi}{\theta} = -1, \tag{14}$$

$$\frac{\phi_\theta}{\phi_x} = \frac{(I + md^2)s^2 + mgd}{mds^2}. \tag{15}$$

The goal of this section was to summarize the tilt-coupling effect in horizontal inertial instruments. It is important to not confuse the tilt coupling induced by gravity with

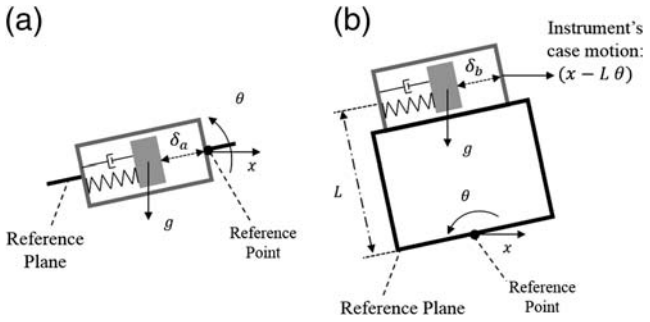

Figure 5. (a) Tilt coupling induced by gravity. (b) Additional geometric coupling related to the separation between the reference point and sensing point.

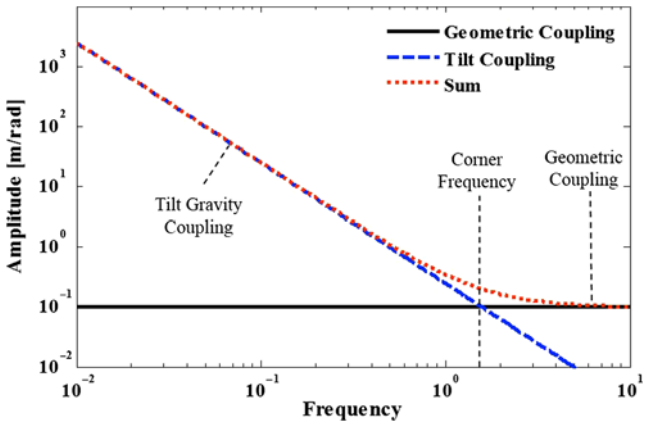

Figure 6. Tilt gravity and geometrical coupling (using $L = 0.1$ m as an example). The color version of this figure is available only in the electronic edition.

the tilt-coupling effect induced by geometrical couplings (angular acceleration). The next section explains the difference between those different types of couplings.

Disambiguation between Tilt-Horizontal Coupling Induced by Gravity and Geometric Cross Coupling (or Angular Acceleration Coupling)

There are several sources of tilt-horizontal couplings. In this section, we classify them in two categories. The first one is related to the effect of gravity on horizontal inertial sensors. This effect was described in the previous section and is the main topic covered in this article. The second category is related to geometrical couplings that arise even in the absence of gravity. These two different effects are illustrated in Figure 5. In this example, the purpose is to measure the translation (x) of a reference location (ground or platform surface) and to quantify the error induced by the tilt effect (θ). The reference location is the point of interest the motion of which must be measured. It can be the ground surface or a particular point on a seismic isolation platform.

- In Figure 5a, the instrument is aligned with the reference plane. The tilt motion will include some error signal through gravity as described in the previous subsection.
- In Figure 5b, the instrument is located at a distance L above the reference plane. The rotation at the reference plane level translates into translation at the sensing point ($-L\theta$). This geometric coupling is in addition to the coupling through gravity.

Equation (16) gives the instrument internal motion δ_a as a function of the input translation and tilt motions for the case described in Figure 5a. Equation (17) gives the instrument internal motion δ_b for the case described in Figure 5b. In the latter, there is an additional term related to the separation L.

$$\delta_a = x\delta_x + \theta\delta_\theta, \tag{16}$$

$$\delta_b = (x - L\theta)\delta_x + \theta\delta_\theta. \tag{17}$$

The horizontal motion can be estimated from the measurement (δ) by dividing the measurement by the instrument translation sensitivity. It is shown in equation (18), in which $\hat{x}$ is the estimated translation motion. In this text, it is referred to as the apparent motion. This estimation is applied to δ_a and δ_b. It produces the apparent motion estimates shown in equations (19) and (20), respectively.

$$\hat{x} = \frac{\delta}{\delta_x}, \tag{18}$$

$$\hat{x}_a = x - \frac{g}{\Omega^2}\theta, \tag{19}$$

$$\hat{x}_b = x - \left(L + \frac{g}{\Omega^2}\right)\theta. \tag{20}$$

Equation (20) includes an extra term ($L\theta$) related to the distance between the reference point and the instrument. The curves in Figure 6 show the tilt sensitivity using the value $L = 0.1$ m as an example. The solid line shows the geometrical coupling term (L), the dashed line shows the gravity coupling term (g/Ω^2), and the dotted line shows the sum of the two terms. At low frequency, the tilt-gravity term (g/Ω^2) dominates. At the frequency Ω_c given in equation (21), tilt gravity and geometrical coupling have the same amplitude. It is called the corner frequency in Figure 6. At high frequency, the geometrical coupling is the dominating term. If L is negative, there is a notch in the response at the corner frequency.

$$\Omega_c = \sqrt{\frac{g}{|L|}}. \tag{21}$$

In some applications, signal due to geometrical coupling effects may be negligible at all frequencies as it is usually

small in relation to the tilt-gravity couplings at low frequencies, and it is often negligible in relation to the translational signal at higher frequencies. The latter statement is true if the input ground motion is sufficiently high in comparison to the input rotation motion as described in

$$x \gg L\theta. \tag{22}$$

Similar effects exist in pendulum seismometers, as covered by Forbriger (2009), in which the effect of angular acceleration on pendulum seismometers is analyzed, and the relation between reference location and sensitivity to angular acceleration is discussed. Detailed developments on pendulum-types sensors are presented in Peters (2009).

Because geometric coupling effects are often negligible at low frequencies when compared with tilt-horizontal couplings induced by gravity, the next sections focus on the tilt-horizontal couplings induced by gravity.

Tilt-Horizontal Coupling in Translation Stages and Vibration Isolation Systems

Inertial sensors are commonly used in seismic and vibration isolation systems to decouple payload (equipment) motion from ground motion. It is important to distinguish two categories of problems. They are the tilt induced by the system's kinematics and the tilt induced by the ground's motion.

Tilt induced by the system's kinematics is a problem intrinsic to the system. When a stage moves horizontally, it always tends to tilt a certain amount with respect to the reference frame. This cross coupling is related to the system's design. It depends on the mechanical architecture of the system and the servocontrol parameters. There are several ways to reduce this effect. First, the system's architecture (joints, flexures, actuators type, and location…) must be carefully designed to diagonalize the translation and rotation effects. This is symbolically illustrated in Figure 7 for a platform mounted on springs. The horizontal force must be aligned with the static center of stiffness of the platform to minimize the low-frequency cross couplings. Machining tolerances and assembly errors will affect the horizontal actuator location (L) and therefore the tilt-coupling ratio. This problem is discussed in Hardham (2005). Aligning the platform's center of mass with the horizontal actuators plane tends to reduce dynamical cross couplings. When the vertical degrees-of-freedom (DOF) are servocontrolled with high loop gain compensators, the cross couplings may be dominated by the angular misalignment of the vertical relative sensors with respect to gravity. This problem and associated compensation techniques are discussed in Kissel (2010).

Although the ground's translation and tilt motion are not necessarily correlated, the tilt-horizontal coupling ratio is usually a specific characteristic of a given mechanical system. It can be frequency dependent, but the transfer function between the stage's horizontal motion and tilt motion is often

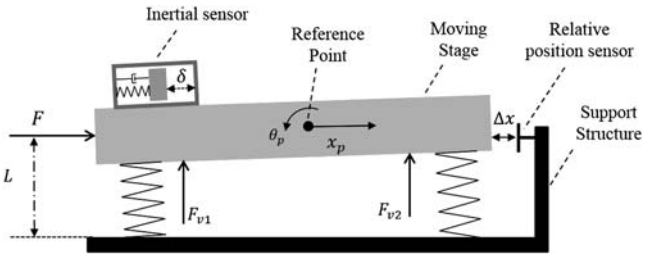

Figure 7. Translation stages with controllable rotational degree-of-freedom (DOF).

mostly linear, and it remains constant over time. It can therefore be identified and suppressed. The low-frequency decoupling can be done using a witness geophone and performing a transfer function as illustrated in Figure 7. The horizontal drive F is used to translate the moving stage. It creates the platform's translation x_p and rotation θ_p. The geophone measurements δ are used to identify the ratio of rotation over translation. Once the cross-coupling value is known it can be minimized in a feedforward manner by applying a torque correction using the forces F_{v1} and F_{v2} as a function of a measurement performed with a relative sensor (Δx). See Kissel (2010) for more details.

When the rotational DOF are not controllable, other techniques must be used. For example, a flexible hinge can be used to transmit the platform motion to the instrument but not the rotation, as illustrated symbolically in Figure 8. The one DOF mechanism must allow horizontal motion with as little tilt as possible. This can be made with a flexure appendage for example. More information on such techniques can be found in Van Eijk *et al.* (2010), Laro *et al.* (2011), or Rijnveld and Van Den Dool (2012). This technique also works for the topology represented in Figure 7.

The active and passive correction techniques discussed in this section show how to reduce the tilt induced by the system's kinematics, but they have no effect on the tilt induced by ground. They suppress the relative tilt induced by translation between the support stage and the moving stage but not the tilt induced by the ground that rotates the support stage.

Isolation performance of vibration isolation platforms can be limited at low frequency by the rotations induced by ground tilt (Lantz *et al.*, 2009). Sensor noise (in vertical instruments and rotations sensors) is the main factor limiting the ability to resolve ground (or platforms) tilt motion. The next two sections are dedicated to this topic.

Sensor Noise and Tilt Coupling

Sensor noise is a key parameter of the tilt-sensing and tilt-subtraction problems. If sensor noise is ignored, the problem becomes trivial because any pair of vertical sensor or any rotation sensor relatively insensitive to translation can apparently be used to measure tilt and subtract it from the horizontal instrument signal. This section discusses some basics

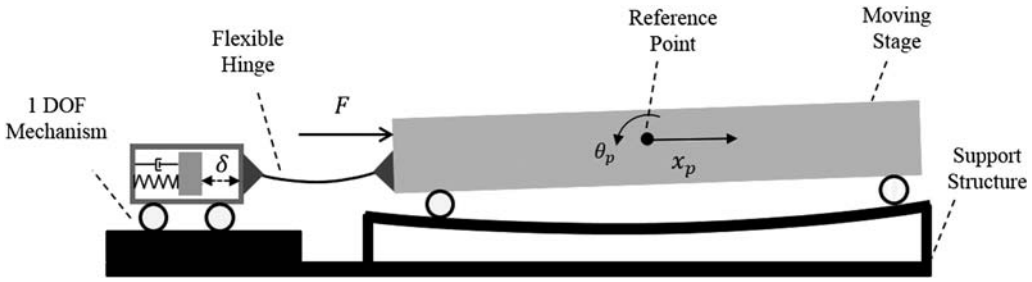

Figure 8. A solution for translation stages with noncontrollable rotational DOF. See Van Eijk *et al.* (2010), Laro *et al.* (2011), and Rijnveld and Van Den Dool (2012) for details on such concepts.

of sensor noise and calibration concepts. The following section will use these concepts and notations to emphasize how sensor noise in vertical instruments and rotation sensors limit the ability to resolve tilt.

Instrument signals are contaminated by several sorts of noise. They can be grouped into two categories. The first group of noise sources is related to environmental disturbances such as ambient pressure, temperature, and magnetic fields. These effects are discussed in Wielandt and Streckeisen (1982) for the force feedback broadband seismometer and more generally in Wielandt (2012). The analysis of the self noise of such instruments remains a topic of great interest (Sleeman and Melichar, 2012). Although Forbriger *et al.* (2010) focuses on low-frequency sensitivity to magnetic fields, the article also provides useful information regarding sensitivity to other environmental disturbances such as temperature and pressure variations. It emphasizes the need for shielding and describes shielding techniques. When measurable, the disturbances can be subtracted from the signal. In this article, we assume that the instrument is perfectly shielded against environmental noise sources (though we know this is not a trivial problem), and we focus only on the tilt coupling that is often a dominant disturbance at low frequencies.

The second group of noise problems is related to stochastic noise sources such as self noise, electronics, and digitization noise inherent to the sensor itself and the data acquisition system. It includes the thermal noise in the mechanical oscillator (Saulson, 1990), sensor readout noise (see, Rodgers, 1993, for electromagnetic readouts or Zumberge *et al.*, 2010, for optical readouts), actuation noise of force balanced instruments (Wielandt and Streckeisen, 1982), and quantization noise (Sleeman *et al.*, 2006). Although the statistical distribution of these noise sources can be estimated or measured, the signal they produce in the time domain cannot be predicted. These noise sources therefore put a limit on the instrument resolution. In the rest of the article, we will call sensor noise the total of those stochastic noise sources.

To relate the tilt-coupling problem to sensor noise, we use the geophone model presented in the previous sections. Recall that δ is the relative motion between the case and the proof-mass of the instrument. This motion is converted to a voltage using an electromechanical converter. It usually uses a coil-magnet system, which produces a signal proportional to velocity. As previously discussed, the developments are done in displacement units, but the analysis and conclusions are the same for a velocity or an acceleration readout. In equation (23), u is the sensor signal in the Laplace domain. The transfer function $H(\mathrm{s})$ is the readout sensitivity $[V/m]$. It includes the electromechanical converter and the entire conditioning chain (preamplifiers, amplifiers, whitening, and antialiasing filters). The noise (in volts) is noted n. It includes the instrument self noise and the electronics chain noise. Equation (24) recalls the transfer function between the relative motion δ and the input motion x. The electromechanical response in equation (23) and the mechanical response in equation (24) are combined to produce the calibration filter C in equation (25):

$$u = \mathrm{H}(s)\delta + n, \tag{23}$$

$$\delta_x = \frac{s^2}{s^2 + 2\mu\omega_s s + \omega_s^2}, \tag{24}$$

$$C = (H\delta_x)^{-1}. \tag{25}$$

The calibrated measurement is obtained as shown in equation (26). The apparent motion ($\hat{x}$) can be expressed as a function of the input translation, the input tilt, and the calibrated noise n_c as shown in equation (27). The latter is the noise calibrated in displacement units as shown in equation (28). In the following sections, we will use this calibrated noise (instead of the noise in volt units), because it can conveniently be compared with the displacement motion as they are in the same units.

$$\hat{x} = Cu, \tag{26}$$

$$\hat{x} = x + \frac{g}{s^2}\theta + n_c, \tag{27}$$

$$n_c = C(s)n. \tag{28}$$

This section emphasized that sensor noise is a very important component of the tilt reconstruction and subtraction problem. The next sections review instruments configurations for tilt subtraction and relate them to sensor noise limitations.

Multiple Instruments Configurations to Subtract Tilt

There are many ways to separate tilt from translation contributions using various combinations of instruments (Bradner and Michael, 1973; Graizer, 1991; Wielandt and Forbriger, 1999; Forbriger, 2009; or Graizer, 2009). Combination of multiple measurements and subtraction techniques require low-noise instruments to separate translation and tilt motion with accuracy. To illustrate this, we use a combination of two vertical seismometers as an example to relate the tilt-gravity coupling problem to sensor noise. We then provide an estimate of the tilt-sensing resolution that can be achieved with a platform equipped with three broadband instruments. We follow up with a review of low-noise rotation sensors.

Example Using Two Vertical Instruments

A pair of vertical geophones is shown in Figure 9 as a basic example to illustrate how multiple sensors can be used to resolve ground tilt to the limit of the sensor noise. The reference point of the ground (or support structure) is subjected to translation x and tilt θ. A horizontal and two vertical instruments are located on the ground plane. In this conceptual example, we assume that the ground (support structure) moves as a rigid body in the sensing area where the three sensors are located. We neglect the small vertical distance between the horizontal instrument center and the reference point (geometric coupling). The translational acceleration and tilt motion produce the response of the horizontal instrument (δ). The two vertical instruments are separated by a distance λ. The ground tilt produces motions z_1 and z_2 at the vertical sensors locations. It produces the instruments internal motions ς_1 and ς_2.

Equation (29) gives the apparent motion ($\hat{x}$) that is obtained when calibrating the response (δ) with the instrument's sensitivity (δ_x). It is made of three terms related to the input translation, the input rotation, and the calibrated sensor noise n_x. Equations (30) and (31) give the apparent motion of the vertical instruments ($\hat{z}_1$ and $\hat{z}_2$) obtained when calibrating the vertical instruments response by the geophone response, assuming that the calibration errors are negligible. Assuming the vertical instruments are well leveled, the apparent vertical motion is, to first order, insensitive to tilt. It is only a function of the vertical motions inputs and the calibrated sensor noise (n_{z1} and n_{z2}).

$$\hat{x} = x + \frac{g}{s^2}\theta + n_x, \tag{29}$$

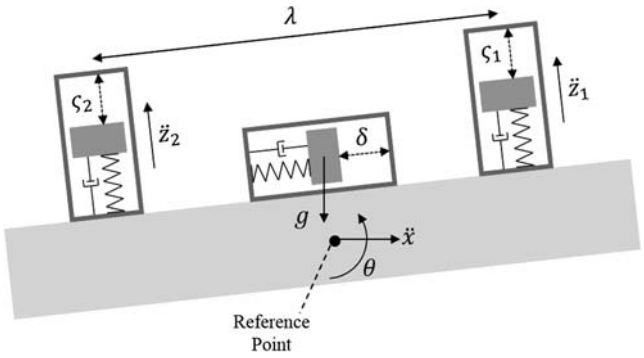

Figure 9. Combining two vertical seismometers to subtract tilt signal from a horizontal seismometer.

$$\hat{z}_1 = z_1 + n_{z1}, \tag{30}$$

$$\hat{z}_2 = z_2 + n_{z2}. \tag{31}$$

Assuming small and rigid body motions, tilt can be estimated as a function of the apparent vertical motion as shown in equation (32). This relation is combined to equation (31) to produce the tilt signal estimate written in equation (33). This tilt estimate is used to subtract tilt from the horizontal measurement as shown in equation (34).

$$\hat{\theta} = \frac{\hat{z}_1 - \hat{z}_2}{\lambda}, \tag{32}$$

$$\hat{\theta} = \frac{z_1 + n_{z1} - z_2 - n_{z2}}{\lambda}, \tag{33}$$

$$\hat{x}_{\text{TiltFree}} = \hat{x} - \hat{\theta}\frac{g}{s^2}. \tag{34}$$

Assuming the two vertical sensors have the same sensor noise amplitude n_z, and that the two instruments noises are completely independent stochastic processes, the tilt-free signal can be written as shown in equations (35) and (36). The noise introduced by the subtraction is noted n_θ. Equation (36) shows the frequency dependence of this noise term indicating that it will likely dominate the tilt-free estimate ($\hat{x}_{\text{TiltFree}}$) at low frequencies.

$$\hat{x}_{\text{TiltFree}} = x + n_x + n_\theta, \tag{35}$$

$$n_\theta \sim \sqrt{2}\frac{g}{\lambda s^2} n_z. \tag{36}$$

Many dedicated instruments and instrumented platforms have the capability to measure both horizontal and tilt motion (Nigbor, 1994; Matichard *et al.*, 2013). We use the first active stage of the LIGO platform shown in Figure 10a to illustrate

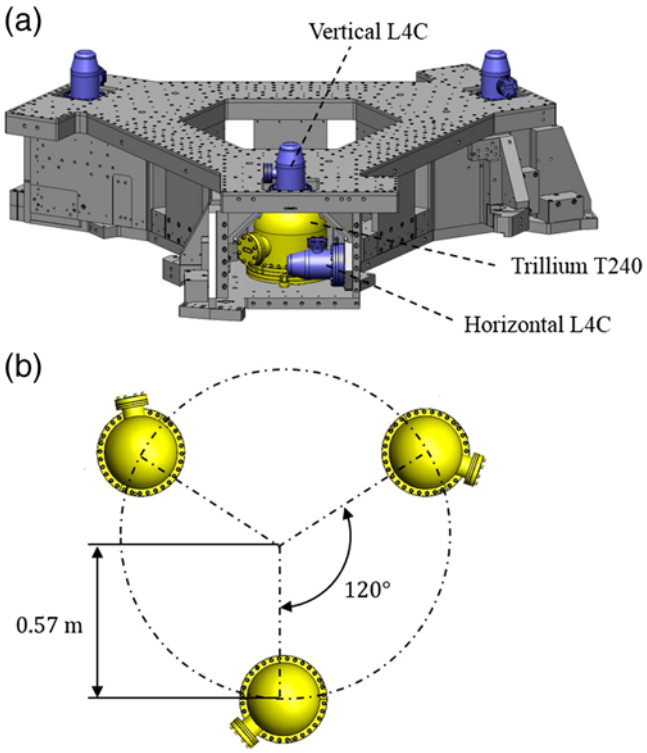

Figure 10. A Laser Interferometer Gravitational-Wave Observatory (LIGO) stage instrumented with three podded three-axis broadband seismometers and six short-period geophones. (a) Oblique view of the structure and instruments. (b) Top view of instruments location (structure not shown). The color version of this figure is available only in the electronic edition.

the sensor noise induced by the tilt subtraction (n_θ). A detailed description of this system is given in Matichard *et al.* (2012). It is instrumented with three broadband seismometers Trillium T240s and with six geophones Sercelle L4Cs. The instruments are podded in sealed chambers to operate in an ultrahigh vacuum environment. The instruments signals are combined (sensor fusion) to produce broadband low-noise signal (Hua *et al.*, 2004; Kissel, 2010; Matichard *et al.*, 2010). The broadband seismometers dominate the sensor fusion at low frequencies and are used here to estimate the tilt motion. The top view in Figure 10b shows the relative location of the three instruments. They are positioned 120° apart on a 0.57 m radius (called r in the following equations).

The vertical instruments are used to subtract tilt from the horizontal measurements as described in equations (33) and (34). It produces an apparent motion ($\hat{x}_{\text{TiltFree}}$), as given in equation (35), that contains a noise term (n_θ), as given in equation (36). The distance between two instruments is given in equation (37). It is combined with equation (36) to obtain the tilt noise given in equation (38), in which the b subscript indicates broadband vertical seismometers have been used for the tilt subtraction.

$$\lambda = 2r\cos\left(\frac{\pi}{6}\right), \tag{37}$$

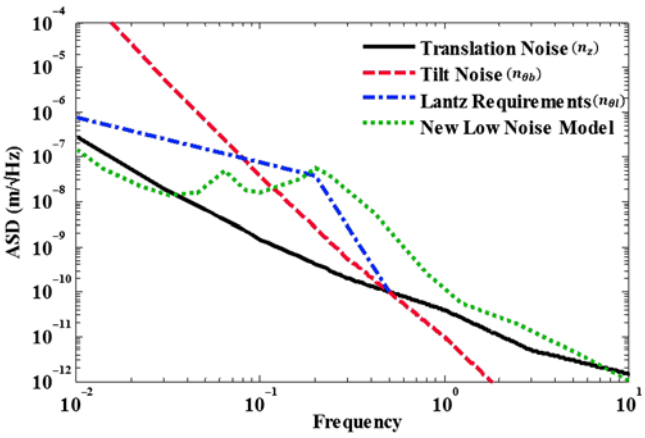

Figure 11. Comparison of amplitude spectral densities of instruments noise models and ground-motion models. The color version of this figure is available only in the electronic edition.

$$n_{\theta b} = \sqrt{\frac{2}{3}}\frac{g}{rs^2}n_z. \tag{38}$$

In the past years, the requirements proposed by Lantz *et al.* (2009) have often been cited as a goal for the development of low-noise tilt sensors, therefore we use them as a reference in this section. A tilt sensor operating at these requirements and used to subtract tilt from a horizontal measurement would produce a noise (apparent horizontal motion) as shown in equation (39), in which the *ts* subscript indicates a tilt sensor operating at Lantz requirements has been used for the tilt estimation. This equation can also be seen as a translation of Lantz requirements to apparent horizontal motion.

$$n_{\theta l} = \frac{g}{s^2}n_{ts}. \tag{39}$$

The plot in Figure 11 shows amplitude spectral densities in displacement units [m/$\sqrt{\text{Hz}}$]. The solid curve shows a model of the self noise of a broadband seismometer (n_z). The dashed curve shows the sensor noise introduced by the tilt subtraction using the vertical broadband seismometers channels ($n_{\theta b}$). The dashed-dotted curve shows the sensor noise introduced by the tilt subtraction using a tilt sensor operating at Lantz requirements ($n_{\theta l}$). The dotted line shows the New Low Noise Model (NLNM) in displacements units (Peterson, 1993). The subtraction using the broadband seismometers meets Lantz requirements down to 90 mHz. Below that frequency, the noise term grows steeply because of the double integration performed during the subtraction process. A tilt sensor operating at Lantz requirements used for tilt subtraction would mask motion at the NLNM level at all frequencies below 180 mHz.

This section highlighted the theoretical limitations of subtraction techniques related to sensor noise. The next subsection reviews recent progress in low-noise tilt instrumentation.

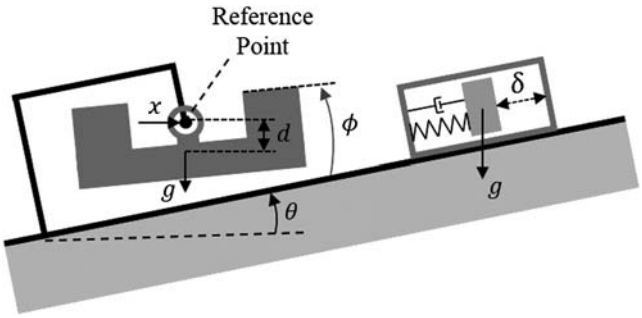

Figure 12. Using a rotation sensor to estimate and subtract tilt.

Using Very Low Noise Rotation Sensors

Using rotation sensors is one of the many possible configurations that can be used to estimate and to subtract tilt from a horizontal measurement. A special issue on rotational seismology was presented by Lee *et al.* (2009). Laser ring gyroscopy is an emerging technology in low-noise rotation seismometry (Lee *et al.*, 2009; Schreiber *et al.*, 2009; Schreiber and Wells, 2013). It is increasingly used in seismology (Igel *et al.*, 2007). Several recent low-noise sensor projects aiming at measuring tilt are based on the beam balance principle as illustrated in Figure 12. The output signal (ϕ) of the beam balance is used to estimate the ground's tilt motion (θ) and subtract it from a horizontal measurement (δ). The tilt estimate must be relatively insensitive to translational acceleration, and it must be very low noise.

The rotation sensor measures the relative angular motion (ϕ) between the beam and the ground. Such instruments can use hinges, knife edges, or flexures to make the articulated joint. We introduce a restoring torque in the joint as shown in equation (40), in which k is the linear angular stiffness. More detailed models can include viscous damping, friction, and hysteresis effects, but it is not necessary for the purpose of this discussion. The beam's relative angular motion induced by the ground translation is shown in equation (41), in which d is the distance between the joint and the center of mass, m is the mass, and I is the inertia at the center of mass. The beam's relative angular motion induced by the ground rotation is shown in equation (42).

$$\tau = -k\phi, \tag{40}$$

$$\frac{\phi}{x} = \frac{-mds^2}{(I + md^2)s^2 + mgd + k}, \tag{41}$$

$$\frac{\phi}{\theta} = \frac{-(I + md^2)s^2 - mgd}{(I + md^2)s^2 + mgd + k}. \tag{42}$$

Below the resonant frequency, the translation and rotation sensitivity can be approximated as shown in equations (43) and (44). The ratio of sensitivities is still equal to g/s^2.

$$\frac{\phi}{x} \sim \frac{-mds^2}{mgd + k}, \tag{43}$$

$$\frac{\phi}{\theta} \sim \frac{-mgd}{mgd + k}. \tag{44}$$

Above the resonant frequency, the translation and rotation sensitivity can be approximated as shown in equations (45) and (46), assuming d is small. The ratio of sensitivities is not any more frequency dependent. It can be tuned as a function of the mass, inertia, and center of mass of location to reduce the translational sensitivity.

$$\frac{\phi}{x} \sim \frac{-md}{I}, \tag{45}$$

$$\frac{\phi}{\theta} \sim -1. \tag{46}$$

The use of rotation sensors to resolve tilt in horizontal inertial measurements has been discussed and investigated since the nineteenth century. Wielandt and Forbriger (1999) recounts how Schluter and Wiechert used a balanced pendulum insensitive to translation (that they called a klinograph) in 1899 to make a direct measurement of tilt. The instrument provided useful insight regarding the contribution of tilt couplings in teleseismometry. This is still a topic of interest more than a century later. Peters (2009) details how to reduce translation sensitivity of a beam balance by aligning the center of mass with the pivot point. Two highly sensitive instruments based on this concept are discussed in this subsection.

It is important to emphasize that the ratio of sensitivities implies that the rotational signal must be time integrated before subtraction from the translational signal. Assuming the rotation and translation sensors are in the same time derivative units (e.g., [rad] and [m] or [rad/s] and [m/s]), a double-time integration of the rotation signal must be performed before subtraction. This results in integration of the intrinsic noise of the rotational signal. It puts constrains on the tilt sensor noise requirements. Tilt sensing requirements, concepts, and experimental tests for gravitational waves detectors are presented in Winterflood *et al.* (2000). The need for tilt sensors for the seismic isolation of gravitational waves detectors recently has driven significant advances in the field of low-noise rotation seismometry.

Venkateswara *et al.* (2014) presented a rotation sensor based on a meter-scale beam balance. The alignment of the center of mass with the balance pivot point reduces the acceleration sensitivity to a very low level (3×10^{-5} rad/m). A high-sensitivity autocollimator is used for the readout. Measurements performed in a vacuum show that the instru-

ment meets Lantz requirements above 30 mHz (sensitivity better than 10^{-9} rad/$\sqrt{\text{Hz}}$).

Dergachev *et al.* (2014) presented a rotation sensor made of a balance. Unlike Venkateswara who uses flexures in the joints, Dergachev uses a knife edge as the pivot. Linear variable differential transformer sensors are used for the readouts. Sensor noise measurements show that the sensitivity of the instrument meets Lantz requirements between 40 and 300 mHz (sensitivity better than 7×10^{-10} rad/$\sqrt{\text{Hz}}$ at 100 mHz). Technical information about this system is provided in O'Toole *et al.* (2014).

The recent progress in rotation seismometry is remarkable. It illustrates the technical challenges to achieve very low noise performance at low frequencies (for instance, between 10 and 100 mHz in the context of seismic isolation for gravitational waves observatories). The use of these instruments will most likely lead to advances in seismometry and seismic isolation. Subtraction techniques require the use of sophisticated auxiliary instruments to make a low-noise estimate of ground tilt to subtract it from a horizontal measurement. In the next section, we discuss the use of suspension mechanisms to produce measurements independently of the support frame.

Suspension Mechanisms

Articulated systems using proof masses with large rotational inertia (called suspensions in this section, and publications cited) can be tuned to act as filters of motion transmission: above the rotational natural frequency of the system, the transmission of rotation to the proof mass can be mechanically filtered by inertial decoupling, whereas translation may remain transmitted in a certain bandwidth upon conditions discussed in the following paragraphs. Although a similar decoupling principle is used in beam balances to measure ground tilt with minimal contribution of the translation input (thanks to a differential angular readout, see previous section), it can also be used to measure linear acceleration with reduced contribution of the tilt input as discussed in this section. For that, the readout must be performed independently of the frame of the instrument, which is rotating with the ground. It should be emphasized that the rotational acceleration of the support structure still couples into linear acceleration through geometrical couplings. The smaller the separation between the reference point and the measurement point, the smaller this coupling (see the Disambiguation between Tilt-Horizontal Coupling Induced by Gravity and Geometric Cross Coupling (or Angular Acceleration Coupling) section).

In this section, we review concepts of sensors that can produce a measurement independent of the frame of the instrument. The basic principles can be illustrated as shown in Figure 13a. A rigid body is suspended with a link of length l. The rigid body has a mass m and inertia I at its center of mass. The center of mass is located at a distance d below the bottom suspension joint. The mass and inertia of the link

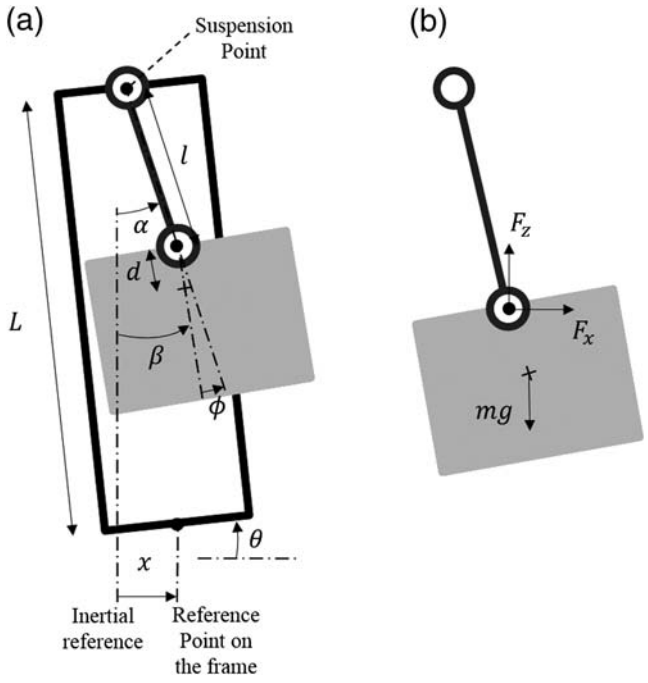

Figure 13. Suspended body parameters and equilibrium.

can be neglected for the purpose of this analysis. The joints can be made with a hinge, flexure, or metal wires. In this introductory example, the suspension joints are considered perfect (no stiffness, no friction). In practice, the joints' stiffness and friction induce coupling between the rotation of the frame and the rotation of the links. The input ground tilt is called θ, the input translation is x, the angle of the link with respect to gravity is α, the angle of the rigid body with respect to gravity is β. As in the previous sections, the geometrical coupling induced by the separation between the reference point and the measurement point must be discussed. The reference point is the point the inertial motion of which must be measured. The separation (L) couples tilt into translation of the suspension point, which is inevitably sensed by the inertial sensor. The translation and rotation of the reference point combine into translation of the suspension point. The instrument will not be able to separate these two contributions.

The motion of the center of mass is given as a function of the imposed motion and the DOF in equation (47). The forces on this body are shown in Figure 13b. The equations of motion are given in the system in equations (48).

The system exhibits two natural frequencies. Equation (49) gives an approximation of the tilt frequency (ω_t), assuming the distance d is small. We will call it the tilt natural frequency because it mostly involves a tilt motion of the suspended mass (β), with very little rotation of the link ($\alpha \ll \beta$). The greater is the inertia of the mass, the lower is the tilt natural frequency. The approximation in equation (50) gives the second natural frequency assuming the distance d is small. It is mostly related to the link's length similar to a

Table 1
Simulation Parameters

Symbol	Name	Value
l	Pendulum length	0.1 m
d	Distance between the bottom joint and the center of mass	0.001 m
m	Suspended mass	10 kg
I	Inertia at the center of mass	1 kg m^2
g	Acceleration of gravity	9.81 m/s^2

point mass pendulum. We will call it the pendulum natural frequency (ω_p).

$$x_g = x - L\theta + \alpha l + \beta d, \tag{47}$$

$$\begin{bmatrix} l & d \\ 0 & I \end{bmatrix} \begin{Bmatrix} \ddot{\alpha} \\ \ddot{\beta} \end{Bmatrix} + \begin{bmatrix} g & 0 \\ -mgd & mgd \end{bmatrix} \begin{Bmatrix} \alpha \\ \beta \end{Bmatrix} = \begin{Bmatrix} -\ddot{x} \\ 0 \end{Bmatrix} + \begin{Bmatrix} L\ddot{\theta} \\ 0 \end{Bmatrix}, \tag{48}$$

$$\omega_t \sim \sqrt{\frac{mgd}{I}}, \tag{49}$$

$$\omega_p \sim \sqrt{\frac{g}{l}}. \tag{50}$$

The DOF α and β can be combined to produce a measurement of the suspension's point translational motion, as given in equation (51), in which ϕ is a measure of the relative angle between the two DOF. There are in theory many other ways to combine these two DOF to provide the readout. In this section, we only analyze the case described by equation (51) to illustrate the principle. For that, we define parameters as shown in Table 1.

$$\phi = \alpha - \beta. \tag{51}$$

The frequency response of the system to the input motion x is shown in Figure 14 for this set of parameters. The solid line shows the amplitude of the transfer function of the link's angle (α/x). The dotted line shows the suspended body's angle (β/x). The dashed line shows the sensor's transfer function (ϕ/x). The response to the input motion θ (not shown) is simply scaled by a factor L. The smaller is L, the smaller the transfer function.

Below the tilt frequency, the angle of the link (α) and the angle of the suspended mass (β) are in phase, and the instrument response (ϕ) is small (function of the fourth power of frequency); but above the tilt frequency, the suspended mass is inertially decoupled, as shown by the gray curve. Its frequency response is flat (md/I) until the pendulum frequency,

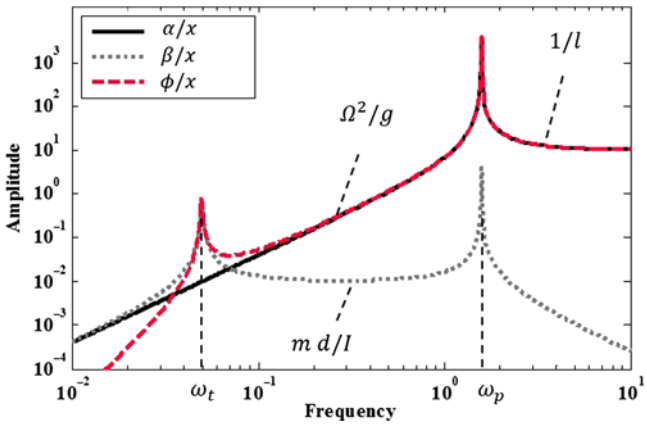

Figure 14. Frequency response to ground translation. The color version of this figure is available only in the electronic edition.

after which it is further decoupled from the input motion. The suspended mass provides an inertial reference to measure the link angle α. The ratio of the solid line (α) over the dotted line (β) increases with the square of frequency as shown in equation (52). The sensor (dashed line, measurement ϕ) provides an inertial measurement of the pendulum response as shown in equation (53). Below the pendulum frequency, the instruments sense the instrument acceleration (s^2/g), as indicated on the plot. This measurement of the translation of the suspension point is performed independently of the frame, which is directly tilting with the ground. Only the tilt contribution through the geometrical coupling remains, as given in equation (54).

For $j\omega_t < s$:

$$\frac{\alpha}{\beta} \sim \frac{s^2}{\omega_t^2}, \tag{52}$$

$$\frac{\phi}{x} \sim \frac{-s^2/l}{s^2 + \omega_p^2}, \tag{53}$$

$$\frac{\phi}{\theta} \sim L\frac{s^2/l}{s^2 + \omega_p^2}. \tag{54}$$

There are many options to engineer the suspensions joints. Detailed analysis on flexure joints can be found in Smith (2000) or Trease *et al.* (2005). The latter focuses on large displacement but provides a detailed review of standard solutions. Using metal wire suspensions is another option. Robertson *et al.* (1982), for instance, proposed to suspend a body near its center of mass to provide an inertial reference for true horizontal motion sensing. More recently, Giazotto (2012) proposed a concept using a suspended mass and force feedback to measure independently horizontal motion and tilt motion. In this particular application, the suspension point can be positioned close to the reference point,

which minimizes the geometrical coupling between the input tilt and the motion of the suspension point.

Conclusion

The article reviewed problems induced by tilt coupling in seismological studies and active seismic isolation applications. It distinguished the different types of couplings that are the tilt-gravity couplings and the tilt-geometric couplings. It discussed problems and solutions related to tilt-gravity couplings in the context of vibration isolation systems and translation stages. It reviewed techniques combining multiple instruments to separate signal due to translation from signal due to tilt. It emphasized the limits related to sensor noise. It used the example of a platform instrumented with three broadband seismometers to illustrate how the sensor noise in vertical channels limits the ability to resolve the platform's horizontal translation motion. It reviewed recent progress in low-noise rotation seismometry. Finally, it discussed the use of suspension mechanisms to filter ground-motion transmission. It highlighted that the use of such sensors can be an alternative to subtraction techniques if the system's natural frequency is properly chosen and if the separation between the reference point and the suspension point is sufficiently small.

Data and Resources

Data used in this study was collected at the LIGO Livingston Observatory. It can be provided upon request.

Acknowledgments

This work was carried out within the Laser Interferometer Gravitational-Wave Observatory (LIGO) laboratory. LIGO was constructed by the California Institute of Technology and Massachusetts Institute of Technology with funding from the National Science Foundation and operates under Cooperative Agreement PHY-0757058. Advanced LIGO was built under Award PHY-0823459. The authors are very grateful to Richard Mittleman, Professor Randall Peters, and an anonymous reviewer for their thorough review of this article. Their comments and suggestions have been very useful. This document has been assigned LIGO Laboratory Document Number LIGO-P1200007.

References

Abbott, R., R. Adhikari, G. Allen, S. Cowley, E. Daw, D. DeBra, J. Giaime, G. Hammond, M. Hammond, C. Hardham, *et al.* (2002). Seismic isolation for Advanced LIGO, *Classical Quant. Grav.* **19,** no. 7, 1591.

Artoos, K., O. Capatina, C. Collette, M. Guinchard, C. Hauviller, F. Lackner, J. Pfingstner, H. Schmickler, M. Sylte, M. Fontaine, *et al.* (2009). Study of the stabilization to the nanometer level of mechanical vibrations of the CLIC main beam Quadrupoles, Number EuCARD-CON-2009-020.

Boroschek, R. L., and D. Legrand (2006). Tilt motion effects on the double-time integration of linear accelerometers: An experimental approach, *Bull. Seismol. Soc. Am.* **96,** no. 6, 2072–2089.

Bradner, H., and R. Michael (1973). Some methods for determining acceleration and tilt by use of pendulums and accelerometers, *Bull. Seismol. Soc. Am.* **63,** no. 1, 1–7.

Collette, C., S. Janssens, K. Artoos, A. Kuzmin, P. Fernandez-Carmona, M. Guinchard, R. Leuxe, and C. Hauviller (2011). Nano-motion control of heavy quadrupoles for future particle colliders: An experimental validation, *Nuclear Instruments and Methods in Physics Research Section A: Accelerators, Spectrometers, Detectors and Associated Equipment* **643,** no. 1, 95–101.

Collette, C., S. Janssens, P. Fernandez-Carmona, K. Artoos, M. Guinchard, C. Hauviller, and A. Preumont (2012). Review: Inertial sensors for low frequency seismic vibration measurement, *Bull. Seismol. Soc. Am.* **102,** no. 4, 1289–1300.

Crawford, W. C., and S. C. Webb (2000). Identifying and removing tilt noise from low-frequency (<0.1 Hz) seafloor vertical seismic data, *Bull. Seismol. Soc. Am.* **90,** no. 4, 952–963.

Dergachev, V., R. DeSalvo, M. Asadoor, A. Bhawal, P. Gong, C. Kim, A. Lottarini, Y. Minenkov, C. Murphy, A. O'Toole, *et al.* (2014). A high precision, compact electromechanical ground rotation sensor, *Rev. Sci. Instrum.* **85,** no. 5, 054502, doi: 10.1063/1.4875375.

Forbriger, T. (2006). Low-frequency limit for H/V studies due to tilt, *Extended Abstract* **32,** 1–4.

Forbriger, T. (2009). About the nonunique sensitivity of pendulum seismometers to translational, angular, and centripetal acceleration, *Bull. Seismol. Soc. Am.* **99,** no. 2B, 1343–1351.

Forbriger, T., R. Widmer-Schnidrig, E. Wielandt, M. Hayman, and N. Ackerley (2010). Magnetic field background variations can limit the resolution of seismic broad-band sensors, *Geophys. J. Int.* **183,** no. 1, 303–312.

Giazotto, A. (2012). Tilt meter as a tilt-independent accelerometer, *Phys. Lett.* **376,** no. 5, 667–670.

Graizer, V. (1991). Inertial seismometry methods, *Izvestiya, Acad. Sci., USSR, Phys. Solid Earth* **27,** 51.

Graizer, V. (2005). Effect of tilt on strong motion data processing, *Soil Dynam. Earthq. Eng.* **25,** no. 3, 197–204.

Graizer, V. (2006). Tilts in strong ground motion, *Bull. Seismol. Soc. Am.* **96,** no. 6, 2090–2102.

Graizer, V. (2009). Review article: Tutorial on measuring rotations using multipendulum systems, *Bull. Seismol. Soc. Am.* **99,** no. 2B, 1064–1072.

Hardham, C. (2005). Quiet hydraulic actuators for LIGO, *Dissertation*, Stanford University.

Hardham, C., B. Abbott, R. Abbott, G. Allen, R. Bork, C. Campbell, K. Carter, D. Coyne, D. DeBra, T. Evans, *et al.* (2004). Multi-DOF isolation and alignment with Quiet Hydraulic Actuators control of precision systems, *Proceedings of ASPE conference on Control of Precision Systems*, Cambridge, Massachusetts, 21–23 April 2013.

Hensley, J. M., A. Peters, and S. Chu (1999). Active low frequency vertical vibration isolation, *Rev. Sci. Inst.* **70,** no. 6, 2735–2741.

Hua, W., R. Adhikari, D. B. DeBra, J. A. Giaime, G. D. Hammond, C. Hardham, M. Hennessy, J. P. How, B. T. Lantz, M. Macinnis, *et al.* (2004). Low-frequency active vibration isolation for advanced LIGO, *Proc. SPIE* **5500,** doi: 10.1117/12.552518.

Igel, H., A. Cochard, J. Wassermann, A. Flaws, U. Schreiber, A. Velikoseltsev, and N. P. Dinh (2007). Broad-band observations of earthquake-induced rotational ground motions, *Geophys. J. Int.* **168,** no. 1, 182–196.

Kalkan, E., and V. Graizer (2007). Coupled tilt and translational ground motion response spectra, *J. Struct. Eng.* **133,** no. 5, 609–619.

Kim, Y., S. Kim, and K. Park (2009). Magnetic force driven six degree-of-freedom active vibration isolation system using a phase compensated velocity sensor, *Rev. Sci. Instrum.* **80,** no. 4, 045108, doi: 10.1063/1.3117462.

Kissel, J. S. (2010). Calibrating and improving the sensitivity of the LIGO detectors, *Dissertation*, Louisiana State University.

Lambotte, S., L. Rivera, and J. Hinderer (2006). Vertical and horizontal seismometric observations of tides, *J. Geodyn.* **41,** no. 1, 39–58.

Lantz, B., R. Schofield, B. O'Reilly, D. E. Clark, and D. DeBra (2009). Review: Requirements for a ground rotation sensor to improve Advanced LIGO, *Bull. Seismol. Soc. Am.* **99,** no. 2B, 980–989.

Laro, D., S. Van den Berg, J. Eisinger, and J. Van Eijk (2011). 6-dof active vibration isolation without tilt-horizontal coupling, *Proc. of the 11th Euspen International Conference*, Como, Iatly, 23–27 May 2011.

Lee, W. K., M. Celebi,, M. I. Todorovska, and H. Igel (2009). Introduction to the special issue on rotational seismology and engineering applications, *Bull. Seismol. Soc. Am.* **99,** no. 2B, 945–957.

Losurdo, G., G. Calamai, E. Cuoco, L. Fabbroni, G. Guidi, M. Mazzoni, R. Stanga, F. Vetrano, L. Holloway, D. Passuello, *et al.* (2001). Inertial control of the mirror suspensions of the VIRGO interferometer for gravitational wave detection, *Rev. Sci. Instrum.* **72,** no. 9, 3653–3661.

Matichard, F., B. Abbott, S. Abbott, E. Allewine, S. Barnum, S. Biscans, D. Clark, D. Coyne, D. DeBra, S. Foley, *et al.* (2013). LIGO vibration isolation and alignment platforms: An overview of systems, features and performance of interest for the field of precision positioning and manufacturing, *Proceedings of ASPE conference on Precision Control for Advanced Manufacturing Systems*, Cambridge, Massachusetts, 21–23 April 2013.

Matichard, F., K. Mason, R. Mittleman, B. Lantz, B. Abbott, M. MacInnis, A. LeRoux, M. Hillard, C. Ramet, S. Barnum, *et al.* (2012). Dynamics enhancements of advanced LIGO multi-stage active vibration isolators and related control performance improvement, *Proceedings of ASME International Design Engineering Technical Conferences and Computers and Information in Engineering Conference*, Chicago, Illinois, 12–15 August 2012.

Matichard, F., R. Mittleman, B. Lantz, B. Abbott, S. Barnum, D. Coyne, D. DeBra, S. Foley, J. Giaime, C. Gray, *et al.* (2010). Prototyping, testing, and performance of the two-stage seismic isolation system for advanced LIGO gravitational wave detectors, *Proc. of ASPE conference on Control of Precision Systems*, Cambridge, Massachusetts, 11–13 April 2010.

Nelson, P. G. (1991). An active vibration isolation system for inertial reference and precision measurement, *Rev. Sci. Instrum.* **62,** no. 9, 2069–2075.

Newell, D. B., S. J. Richman, P. G. Nelson, R. T. Strebbins, P. L. Bender, J. E. Faller, and J. Mason (1997). An ultra-low-noise, low-frequency, six degrees of freedom active vibration isolator, *Revi. Sci. Instrum.* **68,** no. 8, 3211–3219.

Nigbor, R. L. (1994). Six-degree-of-freedom ground-motion measurement, *Bull. Seismol. Soc. Am.* **84,** no. 5, 1665–1669.

O'Toole, A., F. E. Peña Arellano, A. V. Rodionov, M. Shaner, E. Sobacchi, V. Dergachev, R. DeSalvo, M. Asadoor, A. Bhawal, and P. Gong, et al. (2014). Design and initial characterization of a compact ultra-high vacuum compatible low frequency tilt accelerometer, *Rev. Sci. Instrum.* **85,** 075003, doi: 10.1063/1.4890285.

Peters, R. D. (2009). Tutorial on gravitational pendulum theory applied to seismic sensing of translation and rotation, *Bull. Seismol. Soc. Am.* **99,** no. 2B, 1050–1063.

Peterson, J. (1993). Observations and modeling of seismic background noise, 93–95.

Pillet, R., and J. Virieux (2007). The effects of seismic rotations on inertial sensors, *Geophys. J. Int.* **171,** no. 3, 1314–1323.

Pillet, R., A. Deschamps, D. Legrand, J. Virieux, N. Béthoux, and B. Yates (2009). Interpretation of broadband ocean-bottom seismometer horizontal data seismic background noise, *Bull. Seismol. Soc. Am.* **99,** no. 2B, 1333–1342.

Richman, S. J., J. A. Giaime, D. B. Newell, R. T. Stebbins, P. L. Bender, and J. E. Faller (1998). Multistage active vibration isolation system, *Rev. Sci. Instrum.* **69,** no. 6, 2531–2538.

Rijnveld, N., and T. C. Van Den Dool (2012). Active vibration isolation and damping system, *U.S. Patent Application*, 13/377, 402.

Robertson, N. A., R. W. P. Drever, I. Kerr, and J. Hough (1982). Passive and active seismic isolation for gravitational radiation detectors and other instruments, *J. Phys. Sci. Instrum.* **15,** no. 10, 1101.

Rodgers, P. W. (1968). The response of the horizontal pendulum seismometer to Rayleigh and Love waves, tilt, and free oscillations of the Earth, *Bull. Seismol. Soc. Am.* **58,** no. 5, 1385–1406.

Rodgers, P. W. (1969). A note on the response of the pendulum seismometer to plane wave rotation, *Bull. Seismol. Soc. Am.* **59,** no. 5, 2101–2102.

Rodgers, P. W. (1993). Maximizing the signal-to-noise ratio of the electromagnetic seismometer: The optimum coil resistance, amplifier characteristics, and circuit, *Bull. Seismol. Soc. Am.* **83,** no. 2, 561–582.

Saulson, P. R. (1984). Vibration isolation for broadband gravitational wave antennas, *Rev. Sci. Instrum.* **55,** no. 8, 1315–1320.

Saulson, P. R. (1990). Thermal noise in mechanical experiments, *Phys. Rev. D* **42,** no. 8, 2437.

Schreiber, K. U., and J. P. R. Wells (2013). Invited review article: Large ring lasers for rotation sensing, *Rev. Sci. Instrum.* **84,** no. 4, 041101.

Schreiber, K. U., J. N. Hautmann, A. Velikoseltsev, J. Wassermann, H. Igel, and J. Otero, et al. (2009). Ring laser measurements of ground rotations for seismology, *Bull. Seismol. Soc. Am.* **99,** no. 2B, 1190–1198.

Sleeman, R., and P. Melichar (2012). A PDF representation of the STS-2 self-noise obtained from one year of data recorded in the Conrad observatory, Austria, *Bull. Seismol. Soc. Am.* **102,** no. 2, 587–597.

Sleeman, R., A. V. Wettum, and J. Trampert (2006). Three-channel correlation analysis: A new technique to measure instrumental noise of digitizers and seismic sensors, *Bull. Seismol. Soc. Am.* **96,** no. 1, 258–271.

Smith, S. T. (2000). *Flexures: Elements of Elastic Mechanisms*, CRC Press.

Trease, B. P., Y. M. Moon, and S. Kota (2005). Design of large-displacement compliant joints, *J. Mech. Design.* **127,** no. 4, 788–798.

Van Eijk, J., D. A. H. Laro, J. Eisinger, W. W. J. Aarden, and C. J. M. van den Berg (2010). The mythical active vibration isolation, *Proceedings of the American Society of Precision Engineering*, Cambridge, Massachusetts, 11–13 April 2010.

Venkateswara, K., C. A. Hagedorn, M. D. Turner, T. Arp, and J. H. Gundlach (2014). A high-precision mechanical absolute-rotation sensor, *Rev. Sci. Instrum.* **85,** no. 1, 015005, doi: 10.1063/1.4862816.

Wen, S. (2009). Improved seismic isolation for the laser interferometer gravitational wave observatory with hydraulic external pre-isolator system, *Thesis*, Louisiana State University.

Wielandt, E. (2012). Seismic sensors and their calibration, in *New Manual of Seismological Observatory Practice 2 (NMSOP-2)*, P. Bormann (Editor), GeoForschungsZentrum GFZ, Potsdam, Deutsches, 1–51.

Wielandt, E., and T. Forbriger (1999). Near-field seismic displacement and tilt associated with the explosive activity of Stromboli, *Ann. Geofisc.* **42,** no. 3, 407–416.

Wielandt, E., and G. Streckeisen (1982). The leaf-spring seismometer: Design and performance, *Bull. Seismol. Soc. Am.* **72,** no. 6A, 2349–2367.

Winterflood, J., Z. B. Zhou, L. Ju, and D. G. Blair (2000). Tilt suppression for ultra-low residual motion vibration isolation in gravitational wave detection, *Phys. Lett. A* **277,** no. 3, 143–155.

Zumberge, M., J. Berger, J. Otero, and E. Wielandt (2010). An optical seismometer without force feedback, *Bull. Seismol. Soc. Am.* **100,** no. 2, 598–605.

Zürn, W., J. Exss, H. Steffen, C. Kroner, T. Jahr, and M. Westerhaus (2007). On reduction of long period horizontal seismic noise using local barometric pressure, *Geophys. J. Int.* **171,** no. 2, 780–796.

LIGO Project MIT
MIT NW22-295
185 Albany Street
Cambridge, Massachusetts 02139
fabrice@ligo.mit.edu
mevans@ligo.mit.edu

Manuscript received 7 July 2014